ADVANCED FUNCTIONAL MATERIALS
www.afm-journal.de

Materials Views
www.MaterialsViews.com

Uncovering the Structure of Nafion–SiO_2 Hybrid Ionomer Membranes for Prospective Large-Scale Energy Storage Devices

Eric M. Davis, Jenny Kim, Vladimir P. Oleshko, Kirt A. Page, and Christopher L. Soles**

Nafion nanocomposite membranes are attractive candidates for the ion conducting phase in energy storage devices such as vanadium redox flow batteries. Herein, vanadium crossover and Nafion–SiO_2 nanostructure are quantified in a series of hybrid membranes created via solution-casting Nafion films with discrete SiO_2 nanoparticles, as well as membranes created using an in situ silica sol–gel condensation process. The crossover of vanadium ions is suppressed in all Nafion membranes with the SiO_2 inorganic phase when compared to unannealed, neat Nafion membranes. However, it is also observed that annealing the neat Nafion membranes is equally as effective at suppressing vanadium crossover. Small-angle neutron scattering measurements show that no significant changes to the Nafion structure occurred in membranes with discrete nanoparticles. In contrast, drastic changes in the scattering profiles of the Nafion–SiO_2 membranes created via sol–gel chemistry are observed, where the SiO_2 nanoclusters are determined to be on the order of 10 nm in diameter. These scattering length scales are verified through real space images using transmission electron microscopy. Insights from this investigation help elucidate the structure of the Nafion–SiO_2 membranes and suggest that the current hypothesis by how vanadium crossover is reduced may not be fully accurate.

1. Introduction

The vanadium redox flow battery (VRFB) has emerged as a promising electrical energy storage (EES) device for alternative energies (e.g., wind and solar power)[1] due to its long cycle life, flexible design, active thermal management, and fast response time.[2,3] A key part of the VRFB is the ion exchange membrane (IEM), which plays a critical role in battery operation by not only physically separating the anolyte and catholyte solutions but also by providing a medium for ion (charge) transport. The most widely used ionomer for VRFBs is Nafion;[4] a perfluorosulfonic acid membrane that incorporates a Teflon-like backbone with perfluorvinyl ether side-chains terminated by sulfonic acid groups. Nafion membranes are attractive because they integrate high proton conductivity with good chemical and thermal stability.[5] However, Nafion suffers from low ion selectivity which leads to vanadium crossover in the VRFB and decreases energy efficiency of the battery over time.[3]

There have been several efforts to combat the low ion selectivity of Nafion for use as the IEMs in VRFBs. These include creating Nafion blends with other polymers,[6] incorporating inorganic fillers,[3,7,8] layered composites at interfaces,[9–11] as well as synthesizing entirely new classes of Nafion-inspired membranes.[2] More specifically, sol–gel derived Nafion–SiO_2 and Nafion–Si/TiO_2 hybrid membranes were observed to significantly reduce the permeability of vanadium ions and water, while minimally impacting ion exchange capacity (IEC) and proton conductivity, thus improving battery performance.[3,7] It has been suggested that these fillers selectively incorporate into the ion-conducting domains of Nafion, effectively altering (or disrupting) the ion/water transport domains. It is thought that creation of SiO_2 in the ion transport channels acts to reduce vanadium crossover by a "size exclusion" mechanism, impeding the transport of vanadium ions and creating a more ion-selective medium with better crossover resistance. There have been many studies of this type of Nafion–SiO_2 nanocomposite using infrared[12–17] and/or nuclear magnetic resonance (NMR)[14,15,17] spectroscopy to identify the appropriate mechanism and gain a deeper understanding of the local environment of the SiO_2 and Nafion phases. These spectroscopic investigations have provided great insight into the local interactions of the inorganic nanoparticles and the Nafion; however, there is limited information on the nanostructure of these Nafion–SiO_2 composite membranes.

Recently, Ladewig et al.[18] published a structural characterization study of Nafion–SiO_2 nanocomposite membranes created using this sol–gel chemistry approach. They employed both small-angle X-ray scattering (SAXS) and small-angle neutron scattering (SANS) to resolve the structure of the ionic domains in the Nafion composite membranes. While little difference was observed between the X-ray scattering curves of the neat and modified Nafion, SANS showed a broadening and reduction in intensity of the ionomer peak, as well as a slight shift in the ionomer peak position to higher q (i.e., reduction in the d-spacing of this correlation peak, which can be indicative of

Dr. E. M. Davis, Dr. J. Kim, Dr. V. P. Oleshko,
Dr. K. A. Page, Dr. C. L. Soles
Materials Science and Engineering Division
National Institute of Standards and Technology
Gaithersburg, MD 20878, USA
E-mail: eric.davis@nist.gov; christopher.soles@nist.gov

DOI: 10.1002/adfm.201501116

smaller distances between the ionic domains). While this study provided the first experimental evidence that the SiO_2 nanoclusters were forming outside of the ionic domains (e.g., nanoparticles ≥20 nm in diameter were readily observed from transmission electron microscopy (TEM)), these nanoparticles did not show up readily in the SAXS measurements. Furthermore, the SANS measurements did not extend to low enough q to fully capture these larger particles and it remains unclear how the scattering from the semicrystalline nature of the Nafion and the SiO_2 inorganic phases are convoluted in the SANS data.

To further elucidate this issue, we introduce a series of Nafion–SiO_2 hybrid membranes with variations in the type of incorporated SiO_2 to explore the relationship between the structure of the membrane and its resistance to vanadium crossover in a configuration of direct relevance to VRFBs. As a starting point, we prepared the same type of Nafion–SiO_2 hybrid membranes that have been reported elsewhere using a sol–gel chemistry approach.[19] The salient characteristic of this system is that solid Nafion membranes, commercially available, were imbibed with the silicon containing sol–gel precursors and then annealed under conditions where the precursors would react to form solid SiO_2. Under these conditions the morphology of SiO_2 domains evolves in situ as the soaked membrane dries and is thermally annealed. To simplify the process, we also formulated nanocomposite membranes by dispersing discrete SiO_2 nanoparticles (with two different surface treatments) into ethanol-based Nafion solutions and then casting films that dried into solid membranes. In these systems, the morphology of the SiO_2 nanoparticles is predetermined and does not evolve upon drying, although the possibility of forming multiparticle aggregates still exists. The principal characteristic here is that the diameter of the nanoparticle is much larger than the ionic domains of Nafion, meaning that the selective sequestration mechanism discussed earlier is not possible. Vanadium ion crossover was measured using ultraviolet–visible (UV–vis) spectroscopy, while the nanostructure of the fully hydrated, neat and modified, Nafion membranes was measured via SANS. Contrast matching conditions were generated, using a mixture of hydrogenated and deuterated water, to minimize the structural scattering intrinsic to the semicrystalline Nafion, as well as to obtain structural information about the size of the SiO_2 nanoclusters. High resolution TEM (HRTEM) was also employed to corroborate the particle dimensions obtained from scattering. The work presented here suggests that the current hypothesis of how the SiO_2 inorganic phase functions to reduce crossover may not be fully understood.

2. Results and Discussion

In order to better understand the effect of SiO_2 nanoparticle loading on the nanoscale structure of these hybrid membranes, two membrane synthesis routes were pursued. The first of these routes created Nafion–SiO_2 hybrid membranes using a previously established sol–gel chemistry method,[19,20] whereby the SiO_2 inorganic phase is grown directly within a solid (but swollen) Nafion 117 membrane. This presumably leads to a heterogeneous distribution, both in location and size, of SiO_2 nanoparticles in the Nafion matrix. The second uses a solution-casting approach, where both bare (≈20 nm in diameter) and amine surface functionalized SiO_2 nanoparticles (10 nm to 20 nm in diameter) are mixed into a Nafion dispersion (in ethanol) at various concentrations and then solution cast into membranes on quartz windows. This should lead to a well-defined size distribution of SiO_2 particles, predetermined by the size distribution of the initial nanoparticles. In addition, we quantify the effect of thermal annealing of neat Nafion 117 membranes on vanadium crossover.

Figure 1a shows a schematic representation of the diffusion cell used to measure crossover of VO^{2+} ions for both neat and SiO_2 modified Nafion membranes.

The Nafion membrane was sandwiched between two 3 mol L^{-1} sulfuric acid solutions (see Figure 1a), one containing 1.5 mol L^{-1} vanadium(IV) oxide sulfate and the one containing 1.5 mol L^{-1} magnesium sulfate, while the crossover of VO^{2+} ions was quantified with UV–vis spectroscopy. These concentrations represent the same conditions that are of relevance for operating VRFBs. Figure 1b shows the VO^{2+} ion concentration in the receiving solution as a function of time for both the unannealed and annealed Nafion 117, as well as the 10.2% by mass SiO_2 hybrid membrane created using sol–gel chemistry. The time axis has been divided by the membrane thickness squared to eliminate the effect of membrane thickness on the crossover measurements, since the time for vanadium crossover and membrane thickness are coupled.

As qualitatively seen from Figure 1b, the crossover of the VO^{2+} ions is higher for the unmodified, unannealed Nafion 117 membrane than for the SiO_2 nanocomposite membrane

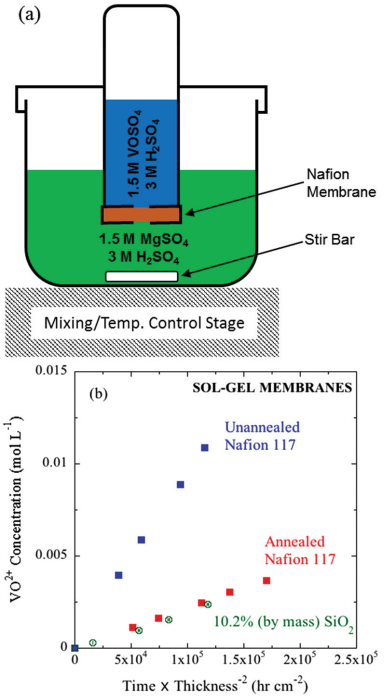

Figure 1. a) Schematic diagram of diffusion cell used to measure VO^{2+} crossover. b) VO^{2+} concentration as a function of time at ≈25 °C for unannealed Nafion 117 (solid blue squares), annealed Nafion 117 (solid red squares), and 10.2% by mass SiO_2 sol–gel membrane (open green circles), measured using UV–vis spectroscopy. Error bars represent propagated error from variations in Nafion film thickness.

over the given experimental time period. A reduction in VO^{2+} crossover between the sol–gel modified and unmodified membranes has previously been attributed to the localization of the SiO_2 nanoclusters inside the water/ion conduction pathways of the Nafion.[3,21] It is commonly believed that SiO_2 nanoparticles form only within the polar, ionic clusters,[12,20,22,23] essentially blocking these water/ion transport channels with an impermeable phase and thus reducing the available volume for vanadium ion transport.[3] While this theory has been actively discussed in the literature, the direct relationship between the role of the inorganic phase and the reduced crossover is still an open discussion. Surprisingly, once the unmodified Nafion 117 membrane is annealed at 140 °C for 2 h, the crossover of vanadium ions is also dramatically reduced and on par with that of the 10.2% by mass SiO_2 sol–gel membrane. The vanadium permeability for these membranes can be calculated using the equation[24]

$$V_B \frac{dC_B}{dt} = A\frac{P}{L}C_A \quad (1)$$

where V_B is the volume of the receiving reservoir, A is the exposed area of the membrane, L is the thickness of the membrane, P is the vanadium permeability, and C_A and C_B are the concentration in the vanadium and receiving reservoir, respectively. There are explicit assumptions that must be noted when using this equation, which include: 1) permeability is independent of vanadium concentration, 2) pseudo-steady state exists in the membrane, and 3) the concentration in the vanadium reservoir is constant.[25] A summary of the vanadium permeability results for Nafion 117 and Nafion–SiO_2 sol–gel membranes is shown in **Table 1**.

Consistent with the trends in Figure 1b, the vanadium permeabilities reported in Table 1 show that vanadium crossover for the both the annealed and sol–gel Nafion membranes are much lower than that of the unannealed Nafion 117 membrane (approximately a fourfold reduction). The vanadium crossover for the unannealed Nafion 117 membrane falls within the range (≈(3 to 6) × 10^{-8} cm^2 s^{-1}) that is reported in the literature,[7,25]

Table 1. Vanadium ion permeability for Nafion and Nafion hybrid membranes created via the sol–gel method. Error bars for the Nafion film thicknesses represent the standard deviation of repeat measurements, while the error for the vanadium permeability are associated with the linear regression of crossover data.

Membrane (–)	Membrane thickness [μm]	Vanadium (VO^{2+}) permeability [×10^{-8} cm^2 s^{-1}]
Unannealed Nafion 117		
Exp. 1	200 ± 1	4.45 ± 0.16
Exp. 2	200 ± 1	4.41 ± 0.28
Annealed Nafion 117		
Exp. 1	200 ± 1	1.08 ± 0.12
Exp. 2	200 ± 1	1.10 ± 0.02
10.2% SiO_2 by mass		
Exp. 1	199 ± 1	0.95 ± 0.08
Exp. 2	199 ± 1	1.07 ± 0.25
Exp. 3	199 ± 1	0.88 ± 0.19

while the value for the sol–gel modified membrane was slightly higher than those reported (≈0.67 × 10^{-8} cm^2 s^{-1}) in the literature. In light of these observations, we point out that much of the current crossover data in the literature compare hybrid Nafion membranes that have been thermally annealed to as-received Nafion 117 membranes that have received no thermal treatment. As shown here, this comparison convolutes two separate effects. Comparing crossover data between samples that have received different heat treatments can be misleading and cause misinterpretations of the mechanism(s) by which crossover is reduced.

To this end, the most interesting result of the vanadium crossover measurements comes from the differences between the unannealed and annealed Nafion 117 membranes, and not between the unannealed Nafion 117 and SiO_2 sol–gel membranes. A major structural difference between unannealed and annealed Nafion 117 is the degree of crystallinity in the membrane, with the annealed version having a higher fraction.[22,26] The simple introduction of more crystallinity has a similar effect to the SiO_2 sol–gel hybrid membrane approach. While this observation does not indicate where the SiO_2 inorganic phase resides within the Nafion matrix, it emphasizes that a similar performance can be obtained without invoking a mechanism by which the SiO_2 selectively sequesters into the ionic domains, thereby reducing crossover.

To further elucidate the mechanism(s) by which the inorganic additives impact the crossover performance, discrete SiO_2 nanoparticles were mixed into Nafion dispersions and solution cast into solid membranes. This membrane synthesis procedure is instructive since the Nafion in solution has more freedom to arrange and dry around the nanoparticles (i.e., interact with the nanoparticles) in a way that is entirely different than the hybrid membranes created via sol–gel chemistry. **Figure 2** shows the VO^{2+} ion concentration in the receiving reservoir as a function

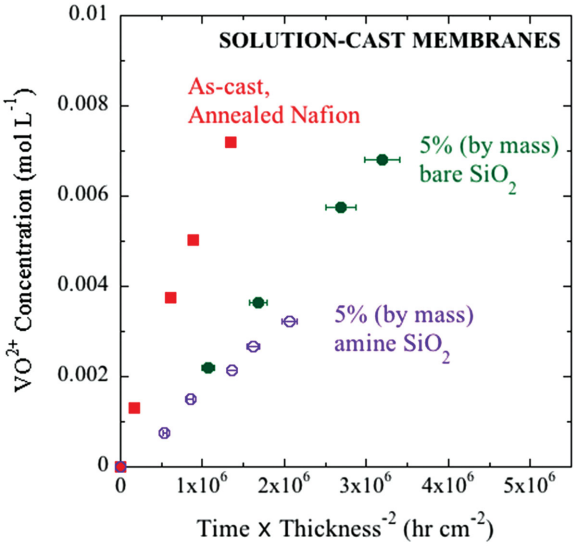

Figure 2. VO^{2+} concentration as a function of time at ≈25 °C for neat, annealed Nafion (solid red squares), 5% by mass bare SiO_2 nanoparticles (solid green circles), and 5% by mass amine-functionalized SiO_2 nanoparticles (open purple circles), measured using UV–vis spectroscopy. Error bars represent propagated error from variations in Nafion film thickness.

Table 2. Vanadium ion permeability for Nafion and Nafion hybrid membranes created via the sol–gel method. Error bars for the Nafion film thicknesses represent the standard deviation of repeat measurements, while the error bars for the vanadium permeability are associated with the linear regression of crossover data.

Membrane (–)	Membrane thickness [μm]	Vanadium (VO^{2+}) permeability [$\times 10^{-8}$ cm^2 s^{-1}]
Solution Cast, Annealed Nafion		
Exp. 1	58 ± 2	0.90 ± 0.11
Exp. 2	55 ± 2	0.78 ± 0.06
5% Bare SiO_2 by mass		
Exp. 1	53 ± 3	0.55 ± 0.07
Exp. 2	40 ± 2	0.50 ± 0.03
5% Amine SiO_2 by mass		
Exp. 1	56 ± 2	0.27 ± 0.02
Exp. 2	24 ± 3	0.40 ± 0.07

of time for both an as-cast, annealed Nafion membrane and hybrid membranes with discrete SiO_2 nanoparticles.

As seen in Figure 2, the crossover of vanadium in the as-cast, annealed Nafion membrane is higher than both the bare and amine-modified SiO_2 nanoparticle solution-cast membranes. It is important to recognize that all membranes in Figure 2 were subjected to annealing at 140 °C for 2 h, so the comparison here does not convolute the effects of thermal annealing with the addition of the SiO_2 nanoparticles. A summary of the vanadium permeability results for these Nafion and Nafion–SiO_2 membranes is shown in **Table 2**.

The vanadium permeability of the as-cast, annealed Nafion membrane is similar to the annealed Nafion 117 membrane (see Table 1); the two different processing routes lead to nominally the same performance. However, there is a reduction in vanadium ion crossover between the SiO_2 loaded (both bare and amine-functionalized) and the as-cast, annealed Nafion membrane (approximately two- to fourfold reduction). The observed reduction in vanadium ion permeability is similar to values reported in the literature for solution-cast hybrid membranes.[25] In many respects it is impossible to invoke a selective sequestration argument here because the SiO_2 nanoparticles are much too large (10 nm to 20 nm in diameter) to solely reside within ion transport channels of the Nafion. Depending on the surface chemistry of the nanoparticles one might expect a selective wetting of the sulfonic groups to the nanoparticle surfaces but at these relatively low loadings, a significant fraction of the native water/ion conduction pathways would remain unchanged. In this respect, it is interesting that relatively large SiO_2 nanoparticles, compared to the dimensions of the ionic transport channels, have what appears to be a greater impact on the vanadium ion crossover than ones created by the in situ sol–gel chemistry approach. These concepts will be explored in more detail below.

In order to gain insight into the nanostructure of these Nafion–SiO_2 hybrid membranes, a series of SANS experiments was performed. **Figure 3** shows the SANS scattering profiles at ≈25 °C of solution-cast, annealed and SiO_2 modified membranes, hydrated in H_2O, with both bare SiO_2 (≈20 nm in diameter) and amine-functionalized SiO_2 nanoparticles (≈10 nm to 20 nm in diameter). Specifically, Figure 3a shows the SANS profiles of solution-cast Nafion membranes with no SiO_2 nanoparticles (red circles), and those membranes loaded with 1% by mass (green squares), 2.5% by mass (purple diamonds), and 5% by mass (blue triangles) bare SiO_2 nanoparticles (i.e., no surface functionalization). The typical scattering pattern for neat Nafion is observed,[27,28] with a low q correlation peak (q = 0.03 to 0.05 Å^{-1}) corresponding to the spacing between crystalline domains of the Teflon-like backbone and a second peak at higher q (q = 0.1 to 0.2 Å^{-1}) corresponding to the spacing between the ionic domains (i.e., sulfonic acid domains; often referred to as the ionomer peak).[29–33] When the bare SiO_2 nanoparticles are added, the position of the low q correlation peak does not measurably shift, although a sharp upturn in the scattering occurs on the lower q side of the peak. This low q upturn is consistent with agglomeration or clustering of the SiO_2 nanoparticles. Additionally, there is no change in the location of the high q correlation peak associated with the ionic domain spacing. This result is further highlighted in Figure 3b, where a close-up of the high q scattering region is shown. These scattering profiles suggest that the introduction of the bare SiO_2 nanoparticles does little to affect the structure of the neat Nafion, where the crystalline and ionic domain spacings of the nanocomposite membranes were independent of SiO_2 nanoparticle loading.

Figure 3c shows the SANS profiles of solution-cast Nafion membranes with no SiO_2 nanoparticles (red circles), and those membranes loaded with 1% by mass (green squares), 2.5% by mass (purple diamonds), and 5% by mass (blue triangles) amine-functionalized SiO_2 nanoparticles. Similar to Figure 3a, the introduction of the amine-functionalized SiO_2 nanoparticles has little effect on the structure of the neat Nafion. A sharp upturn at lower q is quite apparent in these membranes and can again be attributed to clustering of nanoparticles into larger aggregates. The location of the correlation peak associated with the crystalline domain spacing remains constant, while a slight shift to higher q can be observed in the ionomer peak with the highest nanoparticle loading (5% by mass; shown as blue triangles in Figure 3c), possibly suggesting a slight "tightening" of ionic aggregates in the presence of the amine-functionalized surfaces. There also appears to be a slight reduction in the intensity of the high q ionomer peak for the membranes at the loadings of 2.5% by mass and 5% by mass amine-functionalized SiO_2. These subtle variations in the ionomer peak are expanded in Figure 3d, but to a first approximation, the presence of the amine-functionalized SiO_2 nanoparticles does little to affect the nature of the Nafion crystallinity or the ionic aggregates.

One possibility for the slight decrease in peak intensity with the addition of the amine-functionalized nanoparticles is the formation of a water-rich layer at the Nafion/amine-functionalized SiO_2 nanoparticle interface. Both past and current neutron reflectivity work at the National Institute of Standards and Technology (NIST) suggests that a water-rich layer forms at the interface between Nafion and silicon surfaces functionalized with native oxide[34,35] and/or acid-forming amines (NH_3^+). The slight reduction of the ionomer peak intensity observed with loading of amine-functionalized nanoparticles might be consistent with

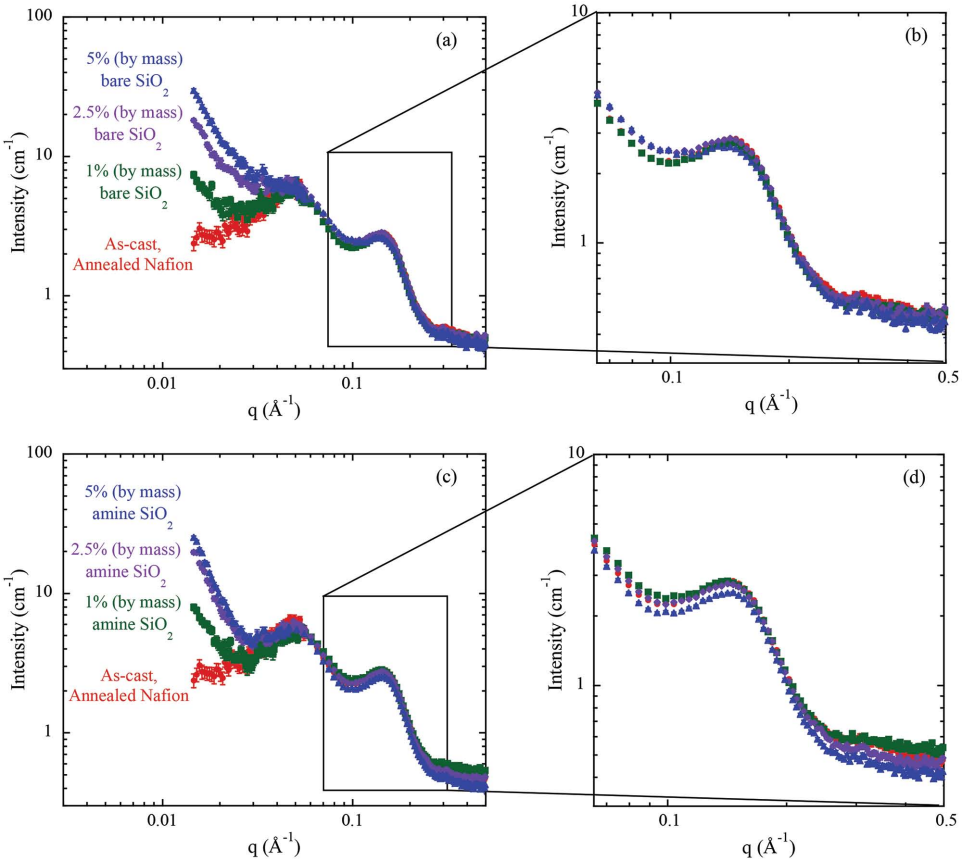

Figure 3. Small-angle neutron scattering (SANS) patterns at ≈25 °C for hydrated (in H_2O) Nafion membranes solution-cast with a) bare SiO_2 nanoparticles, where b) shows a magnification of the high q ionomer correlation peak, and c) amine-functionalized SiO_2 nanoparticles, where d) shows a magnification of the high q ionomer correlation peak.

an interaction between the sulfonic groups and the surface of these particles. This slight interaction with the sulfonic groups may also indicate why crossover of vanadium ions is marginally reduced for these membranes relative to the bare SiO_2 nanoparticle membranes. Again, it must be pointed out that the size of these nanoparticles (≈15 nm in diameter) is much too large for these particles to reside within a single ionic domain. The reduction in vanadium crossover between the as-cast, annealed Nafion and SiO_2 nanoparticle loaded films is similar to the difference in vanadium ion crossover observed between the unannealed and annealed Nafion 117 (three- to fourfold reduction in vanadium permeability). An imperative difference between the two Nafion 117 samples is higher crystallinity (as well as a more dense and compact crystalline phase) for the annealed Nafion 117 membrane. This again emphasizes that performance enhancements can be achieved without selective sequestration of the nanoparticles within the ionic domains. In order to further explore the concept of reduced crossover without preferred sequestration into the ionic domains, SANS measurements of the Nafion sol–gel membranes were performed, where it is thought that formation of the SiO_2 inorganic phase occurs solely within the ionic domain of the bulk Nafion membrane.

Figure 4 shows the hydrated (with H_2O) SANS scattering profiles at ≈25 °C of annealed and SiO_2 modified Nafion 117 membranes created using the sol–gel chemistry approach. Specifically, Figure 4a shows the SANS profiles at ≈25 °C of hydrated (in H_2O) Nafion 117 membranes with no SiO_2 nanoparticles (red circles), and those membranes loaded with 4.8% by mass (green squares), 10.2% by mass (purple diamonds), and 15.9% by mass (blue triangles) SiO_2 sol–gel nanoparticles. Once again a typical scattering pattern is observed for neat Nafion 117, similar to that observed for the solution-cast neat Nafion membrane (see Figure 3a). However, significant differences arise between the scattering profiles of the sol–gel and solution-cast membranes as the SiO_2 content increases. The first of these differences occurs at lower q where the correlation peak associated with the Teflon-like crystalline domains, with a strong maximum at $q \approx 0.02$ Å^{-1}, intensifies and shifts to lower q as SiO_2 loading increases. This broadening appears to occur primarily on the lower q side of the peak (see difference between annealed Nafion 117 and 4.8% by mass SiO_2 sol–gel membrane). At this point is not entirely clear if this reflects a uniform swelling of the Nafion matrix (i.e., pushing the Teflon-like crystalline domains further apart from one another) or the emergence of a new phase associated with the SiO_2 nanoclusters.

The second difference between the scattering profiles of the sol–gel and solution cast membranes occurs at higher q with regards to the correlation peak associated with the sulfonic acid domains. The ionomer peak becomes less distinct as the

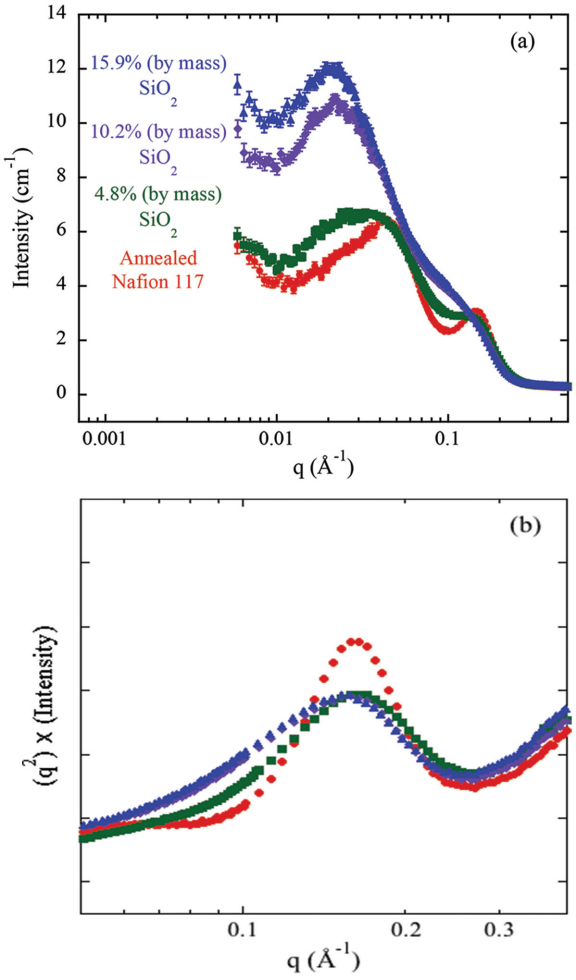

Figure 4. a) Small-angle neutron scattering (SANS) patterns at ≈25 °C for hydrated Nafion 117 (red circles), as well as hydrated Nafion hybrid membranes with 4.8% by mass (green squares), 10.2% by mass (purple diamonds), and 15.9% by mass (blue triangles) SiO_2 nanoparticles, created using sol–gel chemistry. b) Magnification of the high q correlation peak (ionic domains) for Nafion 117 and Nafion hybrid membranes at 25 °C. All membranes were soaked in H_2O for 24 h prior to scattering experiments.

SiO_2 loading increases due to an increase of the scattering intensity on the low q side of the peak. This indicates the possibility of a broadening of the ionic domain distribution within the membrane. To explore this in more detail, Figure 4b expands the high q region of the ionomer peak where the scattering curves have been plotted as (q^2 × Intensity) versus q. This mathematical manipulation serves to minimize scattering at low q, while emphasizing scattering in the high q region. In this representation, a shift of the ionomer peak to lower q upon the impregnation of the SiO_2 sol–gel nanoclusters is not evident; only a marginal shift to lower q is observed for the two highest loadings of 10.2% by mass and 15.9% by mass. This suggests that any SiO_2 nanoclusters formed within the sulfonic acid domains would, to a first approximation, be on the same size or smaller than the sulfonic domains of unmodified Nafion. One would expect the ionomer peak position to change drastically if the introduction of the SiO_2 sol–gel nanoparticles had a significant effect on the ionic structure of Nafion.

In order to better understand where the sol–gel SiO_2 inorganic phase is forming within the Nafion 117 membranes, a series of contrast matching measurements was performed on both the solution-cast and sol–gel SiO_2 membranes. **Figure 5** shows the SANS profiles at ≈25 °C of both as-cast, annealed Nafion and Nafion–SiO_2 solution-cast membranes with 5% by mass bare SiO_2 particles (≈20 nm in diameter), hydrated in both pure H_2O and a mixture of H_2O and D_2O (24/76 by volume). This mixture of protonated and deuterated water creates a solvent environment with a scattering length density of approximately 4.71 × 10^{-10} cm^{-2}, which is similar to the value of 4.54 × 10^{-10} cm^{-2} calculated from the chemical formula of Nafion.[36] Under these contrast match conditions, the scattering length density of the water in the ionic domains will match the scattering length density of the Teflon-like crystallites, reducing the scattering contrast to zero.

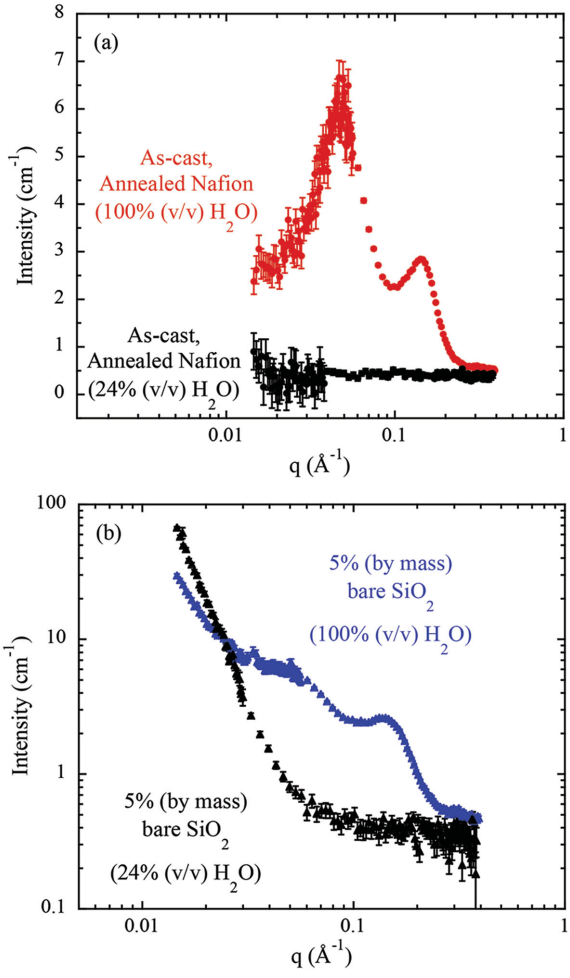

Figure 5. SANS profiles at ≈25 °C of a) as-cast, annealed Nafion membrane in pure H_2O (red circles) and in a 24/76 by volume mixture of H_2O/D_2O (black circles), b) Nafion–SiO_2 solution-cast membrane with 5% by mass bare SiO_2 nanoparticles (blue triangles) in pure H_2O and in a 24/66 by volume mixture of H_2O/D_2O (black triangles).

As seen in Figure 5a, the correlation peaks for the crystalline and ionic domains are completely matched out due to the chosen mixture of protonated and deuterated water in which the Nafion membrane was hydrated (black circles). This result proves that at this H_2O/D_2O ratio the Nafion matrix is essentially invisible to the neutrons, meaning that features in the scattering profiles of the Nafion–SiO_2 solution-cast membranes, soaked in the same H_2O/D_2O solvent ratio, would originate solely from the inorganic SiO_2 phase. Shown in Figure 5b, once the Nafion–SiO_2 solution-cast membrane was soaked in a solvent at the contrast match point of the Nafion matrix, no prominent correlation peaks were observed in the scattering profile. This result is similar to what is observed for the as-cast, annealed Nafion membrane and further highlights that the structure of the Nafion membrane is not significantly altered with the introduction of 5% by mass bare SiO_2 nanoparticles. However, the intensity of the SANS profile of the Nafion–SiO_2 solution-cast membrane with 5% by mass bare SiO_2 nanoparticles begins to increase at q values of about 0.03 to 0.04 $Å^{-1}$. The beginning of this upturn in the scattering data is nominally consistent with the SiO_2 particle diameter of ≈20 nm. Furthermore, at even lower q values, the intensity of the scattering increases more rapidly, which is a result of the density difference between the dense, solid SiO_2 particle and the Nafion. This contrast matching analysis was then extended to Nafion–SiO_2 hybrid membranes created using sol–gel chemistry to gain additional insight into the structure of these nanocomposite membranes. **Figure 6** shows the SANS profiles at ≈25 °C of both pristine Nafion 117 and Nafion–SiO_2 hybrid membranes, hydrated in both pure H_2O and a mixture of H_2O and D_2O (24/76 by volume).

As seen in Figure 6a, there are no prominent correlation peaks in the SANS profile of the Nafion 117 membrane that was soaked in a mixture of H_2O/D_2O at the contrast match point of Nafion (black circles). While there is still some long range heterogeneity that cannot be completely matched out, as evidenced by the sharp upturn seen at lower q, the Nafion 117 membrane is essentially invisible to the neutrons. Again, this means that features in the scattering profiles of the Nafion–SiO_2 hybrid membranes, soaked at this H_2O/D_2O solvent ratio, would originate solely from the inorganic SiO_2 phase. Figure 6b shows the SANS profiles of a Nafion–SiO_2 hybrid membrane with 26.2% by mass SiO_2 loading that was soaked in both H_2O and a mixture of H_2O/D_2O. Interestingly, after the Nafion–SiO_2 membrane was soaked in a H_2O/D_2O mixture at the Nafion contrast match point, a feature in the scattering profile around a q value of 0.02 $Å^{-1}$ is still present. This feature can be seen more clearly in Figure 6c, where the SANS profiles for the series of Nafion–SiO_2 membranes at the Nafion contrast match point are presented.

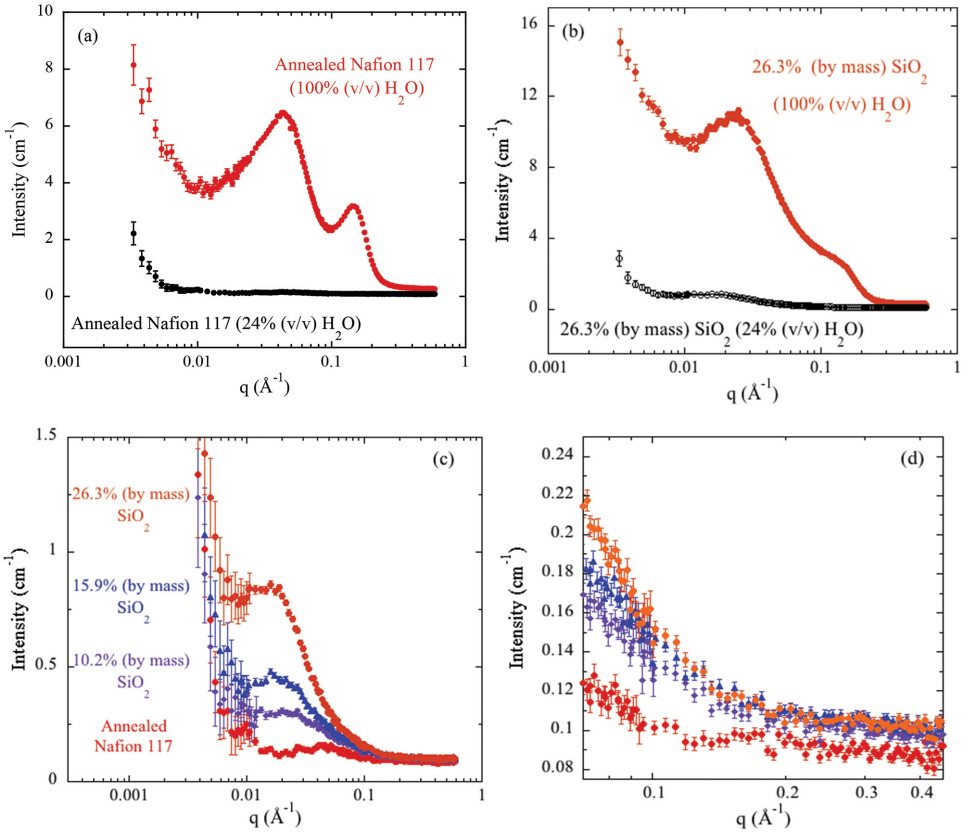

Figure 6. SANS profiles at ≈25 °C of a) Nafion 117 in pure H_2O and in a 24/76 by volume mixture of H_2O/D_2O, b) Nafion–SiO_2 hybrid membrane with 26.3% by mass SiO_2 content (orange circles) in pure H_2O and in a 24/66 by volume mixture of H_2O/D_2O, c) a full series of Nafion–SiO_2 hybrid membranes, and d) a magnification of high q region of the scattering profiles for the same series of Nafion–SiO_2 hybrid membranes in a 24/76 by volume mixture of H_2O/D_2O.

It is clear from Figure 6c that the scattering profiles of the Nafion–SiO_2 hybrid membranes show a peak at $q \approx 0.02$ Å^{-1} that is not present in the neat Nafion 117 sample. This peak represents scattering from the SiO_2 domains that are created in the Nafion 117 during the sol–gel synthesis. Additionally, there is evidence that the SiO_2 nanoclusters in the sol–gel membrane are surrounded by water when the hybrid membrane is hydrated. This is evidenced by the difference in the absolute intensity of the SiO_2 correlation peak of the hybrid membrane hydrated in pure H_2O and in a mixture of H_2O and D_2O. The absolute intensity of the correlation peak shown in Figure 6c is much lower than that shown in Figure 6b (i.e., the difference between the absolute intensity of the orange squares in Figure 6b,c), even if we account for the intensity already present from the neat Nafion 117 membrane. This loss in absolute intensity is due to a loss in contrast between the SiO_2 sol–gel particle and the surrounding matrix, which indicates that the higher absolute intensity observed in Figure 6b is due to the contrast between the SiO_2 sol–gel particle (SLD $\approx 4.2 \times 10^{-6}$ Å^{-2}) and a water-rich layer around the particle (SLD $\approx -0.56 \times 10^{-6}$ Å^{-2}). However, it must be pointed out that the presence of a water-rich layer around the sol–gel particle does not provide evidence for the presence of sulfonic groups around the particle (i.e., this does not prove that ionic domains coalesce around the sol–gel particles). It has been shown that lower molecular weight alcohols (e.g., methanol, ethanol) swell not only the sulfonic (ionic) domains of Nafion but also swell/interact with the ether side chains of Nafion.[37,38] This is important to note since the sol–gel reaction involves equilibrating the Nafion membrane in a mixture of water and methanol, meaning it is likely that additional water is present in these swollen amorphous regions of Nafion, where this additional water could provide the necessary reactant to facilitate the sol–gel reaction.

Furthermore, a comparison of the absolute intensity of the sol–gel membranes to that of the Nafion–SiO_2 solution-cast membrane at the contrast match point can also provide additional insight into properties of the inorganic phase in these sol–gel membranes. Unlike the solution-cast membrane (see Figure 5b; black triangles), the absolute intensity of the sol–gel membrane with 26.3% by mass SiO_2 is only around 1.5 cm^{-1} (almost an order of magnitude lower than the solution-cast film with only 5% by mass SiO_2). This would indicate that the density of the SiO_2 phase in the sol–gel membranes is much less than a monolithic particle of SiO_2. More interestingly, there is no correlation peak present in the high q region where the ionomer peak of Nafion is typically observed. This point is emphasized in Figure 6d, where a magnification of the high q scattering region is presented. One might expect that if the ionic domains of Nafion were used as a template for the growth of the SiO_2 inorganic phase, a correlation peak would be present despite the contrast matching conditions of the water mixture. The fact that there is no correlation peak present in the scattering profile suggests one of three things: 1) SiO_2 is absent from the ionic domains, 2) only a small percentage of the ionic domains contain SiO_2, or 3) only a small percentage of the SiO_2 inorganic phase exists within the ionic domains, where this percentage is small enough that long-range correlations between these smaller nanoclusters are not observed. We will return to this discussion after introducing TEM data later in the paper. In order to determine the size of the SiO_2 inorganic phase for the Nafion sol–gel membranes, the SANS profiles were modeled using a Guinier-Porod analysis to quantify a radius of SiO_2 nanoclusters.

Figure 7 shows the results of the Guinier–Porod analysis for a Nafion–SiO_2 hybrid membrane with 10.2% by mass SiO_2 loading created using the sol–gel chemistry approach.

As seen in Figure 7a, the Guinier–Porod model does an adequate job at parameterizing the scattering profile for the Nafion–SiO_2 hybrid membrane in the range of intermediate q, where the Guinier–Porod analysis is used here as a quick back of the envelop calculation for the relevant length scales. Figure 7b summarizes the radius of gyration for the SiO_2 inorganic phase as a function of SiO_2 loading for the Nafion–SiO_2 sol–gel membranes. The radius of gyration increases from approximately 3 nm at 10.2% by mass SiO_2 loading to approximately 4.5 nm at 26.3% by mass SiO_2 loading. If one assumes that these SiO_2 nanoclusters are spherical, the radius of the inorganic phase can be determined from the radius of gyration through the following relationship, $R_g^2 = 3R^2/5$.

Figure 7c summarizes the radius of the SiO_2 nanoclusters as a function of SiO_2 loading. The solid black lines represent the range of radii that are most widely reported as the size of the sulfonic acid domains in Nafion.[29,33] From this crude estimation it is clear that the radii of the SiO_2 nanoclusters are significantly larger than that of the ionic domains of neat, unmodified Nafion. This is an important finding because again, the most widely accepted theory for the formation of the SiO_2 inorganic phase proposes that these nanoclusters form and reside primarily within the ionic domains of the Nafion. It is thought that this preferential sequestration of the inorganic phase into the ionic domains of the Nafion, essentially "blocking" the vanadium ions from transporting through the ionic channels, is the mechanism by which vanadium crossover is reduced (i.e., steric hindrance of the hydrated vanadium ions). Since the radii of these particles varies from approximately 3.5 nm to 5.5 nm, it is unlikely that all of the SiO_2 nanoclusters reside within the ionic channels of Nafion since this would suggest that the ionic aggregates expand to more than 100% of their current size in the neat, unmodified Nafion. While the formation of some of the SiO_2 nanoclusters within the ionic domains is more than likely occuring, these results suggest that a portion of the SiO_2 inorganic phase resides within the amorphous matrix of the Nafion due to the large size of the nanoparticles. This result also suggests that the current picture of how vanadium ion crossover is reduced may not be completely accurate. Since the SANS data show no changes to the structure of Nafion for the hybrid membranes, it is possible that the introduction of the rigid SiO_2 phase slows down the Nafion chain dynamics (reducing swelling dynamics), which impedes transport and effectively slows the crossover of vanadium ions in these modified membranes. Reduced dynamics have been previously reported for thin Nafion films on SiO_x surfaces,[39] where both reduced water uptake and water diffusivity were observed. Since the silica nanoparticles are simply nanoparticle analogs of these SiO_x surfaces, it is possible that the introduction of the SiO_2 phase creates areas where the Nafion chain dynamics are retarded, ultimately leading to the observed reduction in vanadium crossover.

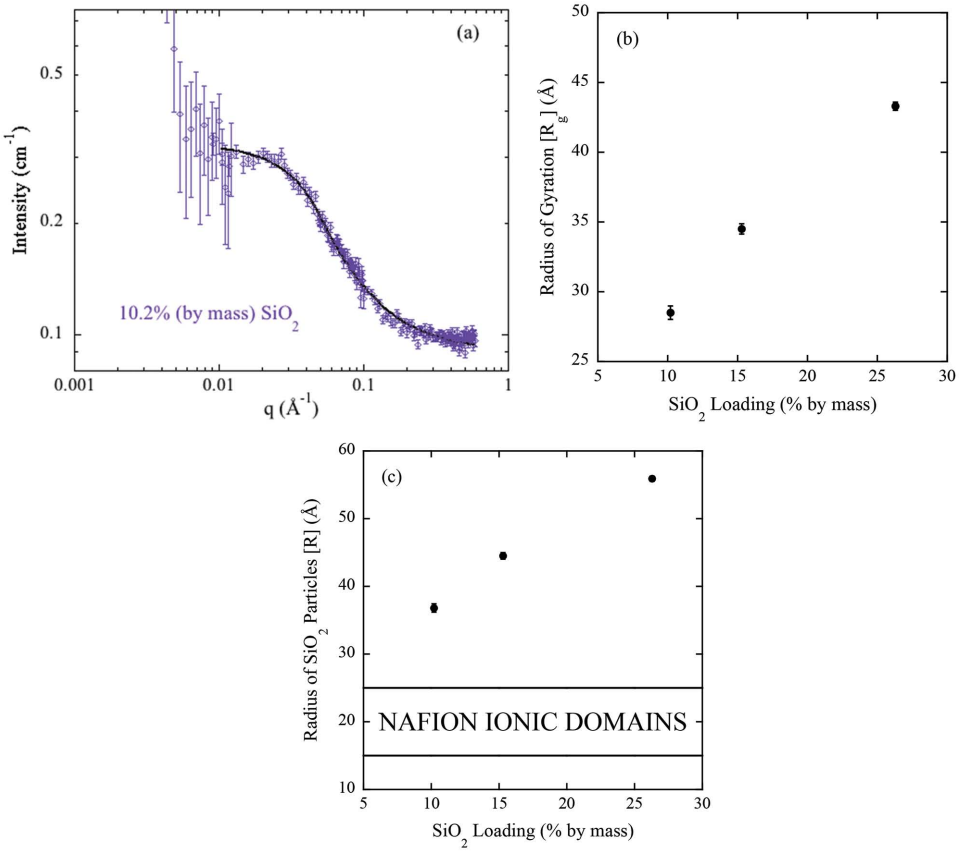

Figure 7. a) SANS profile at ≈25 °C of a Nafion–SiO_2 hybrid membrane with 10.2% by mass SiO_2 loading hydrated with a H_2O/D_2O (24/76 by volume) mixture, where the solid black line is a best fit regression the scattering data to the Guinier-Porod model. b) Radius of gyration of the SiO_2 nanoclusters as a function of SiO_2 loading for Nafion–SiO_2 hybrid membranes. c) Assuming spherical geometry of the nanoclusters, radius of the SiO_2 nanoclusters as a function of SiO_2 loading for Nafion–SiO_2 hybrid membranes. The solid black lines represent the range of ionic domain radii that are most widely accepted for the size of the sulfonic acid bundles. The error bars in (b) and (c) represent the error associated with the model regression.

While information obtained from modeling the SANS profiles can be useful, a real-space image of the SiO_2 nanoclusters to corroborate the SANS results would be ideal. In order to obtain images of the SiO_2 inorganic phase, TEM was employed. **Figure 8** shows the TEM images that were obtained for a Nafion–SiO_2 sol–gel membrane with 10.2% by mass SiO_2 loading. In Figure 8a,b, the dark regions in the BFTEM and HRTEM images represent the SiO_2 inorganic, nanodispersed phase embedded into the Nafion matrix. There appear to be dark SiO_2 nanoclusters ranging in size from approximately 5 nm to several 10s of nanometers. It also appears that these SiO_2 nanoclusters aggregate into diffuse, larger nanoclusters on the order of 100s of nanometers in size. These length scales are completely consistent with the SANS data presented in Figure 7. Additionally, a SAED pattern in Figure 8a (inset) for the 10.2% by mass SiO_2 hybrid membrane displays two broad diffuse rings. These rings are consistent with short-range ordering of the SiO_2 inorganic phase, with the most probable spacing of about 0.21 and 0.11 nm, respectively, superimposed on an amorphous halo, indicating the coexistence of nanocrystallites and largely amorphous regions with no long-range order. According to Yakovlev et al.,[40] these rings are consistent with the (101) and (002) reflections of an orthorhombic polymorph of Nafion. Broadening of the diffraction rings, together with the appearance of the halo, can be associated with short-range ordering of the amorphous Nafion and silica phases (i.e., with roughly uniform interatomic distances as constituent carbon, silicon, and oxygen atoms pack around each other).

The SiO_2 particle size obtained from the TEM images corroborates the Guinier–Porod length scales obtained from the SANS data (on the order of 10 nm in diameter) and is similar to the size of nanoparticles observed by Ladewig et al.[18] on the same material. Figure 8a,b presents a clear picture of how the SiO_2 nanophase exists inside the Nafion 117 matrix, where smaller SiO_2 nanoclusters (2 to 4 nm in diameter) reside inside a small portion of the ionic domains and the larger SiO_2 nanoclusters (>5 nm in diameter) reside inside the amorphous Nafion matrix. To validate the presence of the SiO_2 inorganic phase throughout the entire hybrid membrane, energy dispersive X-ray (EDX) spectroscopy in high-angle annular dark-field scanning TEM (HAADF-STEM) mode was employed. The results of this analysis are presented in Figure 8c,d, where the prominent Si Kα line centered around 1.74 keV shown in Figure 8d is representative of the silica (Si and O) in the SiO_2 nanoclusters. Poor contrast in the TEM images of Figure 8a,b is dictated by the relatively low atomic number and weak electron scattering

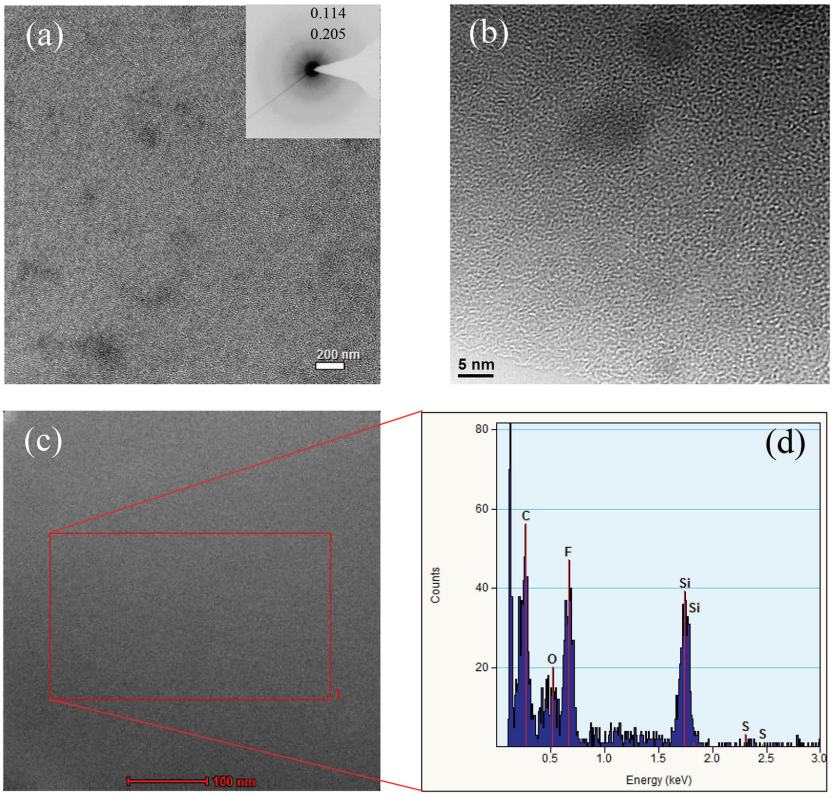

Figure 8. a) Bright-field TEM (BFTEM), b) HRTEM images where the SiO_2 phase is shown by the darker regions, and c) high-angle annular dark-field scanning TEM (HAADF STEM) image and energy dispersive x-ray (EDX) spectrum of a Nafion–SiO_2 hybrid membrane with 10.2% by mass SiO_2 loading. The inset in a) shows corresponding inverted selected-area diffraction (SAED) pattern. The x-ray spectrum has been acquired over area marked by red box in (c) for 60 s. Note that observed x-ray lines belong to both the Nafion matrix (the C Kα line at 0.28 keV, the O Kα line at 0.52 keV (in part), the F Kα line at 0.68 keV, and the minor S Kα line at 2.31 keV), and to the SiO_2 phase (the Si Kα line at 1.74 keV and the O Kα line at 0.52 keV (in part)).

in the materials, as well as its high sensitivity to beam radiation damage.[40] Furthermore, there is little visible contrast in the HAADF-STEM image (see Figure 8c) acquired by collecting high-angle Rutherford scattered electrons, so-called Z-contrast imaging, which is again due to the low variations in the mean atomic number of the constituents in the Nafion–SiO_2 hybrid membranes.

Corroborating the physical picture seen in the TEM images, the EDX indicated the presence of silica (Si and O) over the entire area. This result highlights that silica is present throughout the entire film, meaning that the inorganic SiO_2 phase exists in both the ionic and nonionic (amorphous matrix) of the Nafion 117 membrane, though we can discern from previous scattering results that the SiO_2 phase formed is highly irregular, indicated by the lack of a correlation peak at high q in the contrast matched membranes. Combining the results obtained from the SANS experiments and modeling, along with the images obtained from TEM, a better understanding of the structure of these Nafion–SiO_2 hybrid membranes begins to emerge. It is clear from both experimental techniques that the SiO_2 nanoclusters that are created during the sol–gel process are much too large to solely reside within the sulfonic acid ionic domains of Nafion. This means that the larger, more well-defined SiO_2 nanoclusters exist in the amorphous domains of the Nafion, which brings into the question the mechanism by which vanadium crossover is reduced in membranes that contain the SiO_2 phase, both solution-cast membranes and ones created via sol–gel chemistry. The results of this study are consistent with recent literature, where Dresch et al.[41] observed that the growth of silica particles occurred in both the ionic and nonionic domains of Nafion and was dependent on the solvent media in which the sol–gel reaction was performed. Furthermore, regardless of where the SiO_2 phase resides in the sol–gel hybrid membranes, one possible explanation for the reduced crossover is a decrease in the chain dynamics of the Nafion with the introduction of the SiO_2 nanoparticles, as well as a reduction in chain dynamics with annealing at elevated temperatures (i.e., chain stiffening). In addition to the previously mentioned investigation of Nafion thin films on SiO_x surfaces,[39] a reduction in the local chain dynamics with the introduction of nanoparticles (and small macromolecules) has been previously reported.[42–44] The results of this study highlight the need for additional investigations to elucidate additional (and more accurate) mechanism(s) by which crossover of vanadium ions is suppressed, since it is this reduction in ion crossover that ultimately leads to better battery performance and longer battery life times.

3. Conclusions

In this study, the crossover of vanadium in a number of Nafion–SiO_2 hybrid membranes synthesized using sol–gel chemistry, as well as directly cast from Nafion–SiO_2 dispersions was measured. Vanadium crossover was inhibited in both the solution-cast membranes and the membranes created via sol–gel chemistry compared to pristine, unannealed Nafion. This result is somewhat surprising since the solution-cast membranes contained discrete nanoparticles with diameters much too large to partition into the ionic domains, indicating that suppressed vanadium crossover could be achieved without the SiO_2 nanoparticles "blocking" the transport channels of Nafion. Furthermore, a reduction in crossover was observed for neat Nafion 117 membranes (similar to sol–gel films) that were annealed at elevated temperatures. Additionally, the structure of Nafion–SiO_2 nanocomposite membranes was measured using SANS. Through contrast matching studies of the Nafion membranes, direct information about the SiO_2 inorganic phase was obtained. The SANS profiles were modeled using a Guinier–Porod analysis, where it was determined that the size of these nanoclusters was large enough to suggest that a large portion

of the SiO_2 phase resides within the amorphous matrix of the Nafion membrane. The average size, as well as the elemental composition of the SiO_2 nanoclusters in the Nafion–SiO_2 hybrid membranes were analyzed by TEM coupled with EDX spectroscopic analysis in HAADF-STEM mode. Our results contrast the current hypothesis that these synthesized nanoclusters only exist in the ionic domains of Nafion, suggesting that changes in polymer chain dynamics with the addition of nanoparticles may be an additional mechanism by which vanadium crossover is reduced. These results also emphasize the need for further investigations on Nafion chain dynamics and water/ion transport in these hybrid membranes.

4. Experimental Section

Materials: Tetraethylorthosilicate (TEOS, 98%), methanol (for HPLC, ≥ 99.9%), hydrogen peroxide (30 mass% in H_2O, ACS reagent), sulfuric acid (0.5 mol L^{-1} H_2SO_4 (1.0 N)), deuterium oxide (99.9 atom% D), vanadium(IV) oxide sulfate hydrate (97%), and Nafion stock solution (20 wt% in mixture of lower aliphatic alcohols and water; contains 34%) were purchased from Sigma-Aldrich. Sulfuric acid (≈18 mol L^{-1}, ACS reagent) was purchased from J. T. Baker. Bare silica nanoparticles (SiO_2, 99.5%, 20 nm, nonporous) and amine surface functionalized silica nanoparticles (SiO_2, 99.8%, 10 nm to 20 nm, surface modified with amino group, dispersible) were purchased from SkySpring Nanomaterials, Inc. More detailed information on the specific surface area (SSA) and the nanoparticle size (APS) can be found at the manufacture's website. Nafion 117 (1100 EW, 178 μm (0.007 in.) as-received thickness, commercially extruded film) was purchased from Ion Power, Inc. Deionized water (resistivity ≈18 MΩ cm) was used for all membrane purification and synthesis procedures.

Membrane Purification: Nafion 117 membranes used for SiO_2 sol–gel synthesis were cut into 4 × 9 cm rectangles. All cut membranes were then purified using a method previously developed,[45] by refluxing the membranes in 3 mass% hydrogen peroxide, deionized water, 0.5 mol L^{-1} sulfuric acid, and then finally in deionized water again. Each reflux step was ≈1 h and the Nafion membrane was excessively washed with deionized water after each step. The purified membranes were then dried under vacuum at 90 °C for 24 h to obtained the dry mass (i.e., without SiO_2).

Nanocomposite Membrane Synthesis: Solution-Cast Composite Membranes: The as-received Nafion stock solution was first poured into a Teflon petri dish and heated at 80 °C for 24 h (under vacuum) to evaporate off the solvent mixture. The solid Nafion left over after evaporation was then re-dispersed in pure ethanol for 24 h to create a 10% by mass Nafion dispersion. All subsequent membranes were solution cast from this new Nafion stock solution. To create the Nafion–SiO_2 hybrid membranes, various amounts of SiO_2 nanoparticles (both bare and amine surface functionalized) were suspended in the Nafion stock solution and then directly cast onto quartz windows to be used in SANS experiments. All Nafion–SiO_2 dispersions were sonicated for at least 15 min prior to casting. Additionally, the SiO_2% (by mass) of each solution was calculated in reference to the amount of Nafion (solids) present in the solution volume. The solution-cast hybrid membranes were allowed to dry overnight (≈12 h) and then subjected to annealing at 140 °C for 2 h under vacuum, where afterward, the heat was shutoff and the oven was allowed to cool down to room temperature before films were removed. Solution-cast Nafion–SiO_2 films were on the order of 25 to 50 μm in thickness.

Nanocomposite Membrane Synthesis: Sol–Gel Composite Membranes: Using a method previously developed,[20] the purified Nafion 117 membranes were first equilibrated in a 2:1 (v/v) methanol/water solution for 4 h. The equilibrated membrane was then placed in a stoppered flask containing 50 mL of the same 2:1 methanol/water solution, where immediately afterward, TEOS was introduced in amounts such that water/TEOS = 4:1 (mol/mol). In order to ensure complete alkoxide hydrolysis, the TEOS was added to the flasks in a solution consisting of TEOS/methanol at 1.5:1 (v/v). The reaction vessels were immediately sealed once all liquids were added. The membrane was then removed from the reaction vessels at select time intervals and washed with pure methanol to prevent the formation of the silica phase on the surface of the membrane. Upon removal from the pure methanol wash, the surface of the membranes was blotted dry, and then the films were dried under vacuum for 24 h and subsequently annealed at 140 °C for 2 h, afterwhich, the heat was shutoff and the oven was allowed to cool down to room temperature before films were removed. The membranes were then weighed to determine the mass-loading of the SiO_2 inorganic phase. All steps, excluding annealing, were carried out at room temperature.

Small-Angle Neutron Scattering: Small-angle neutron scattering experiments were performed on the NG-B 10 m SANS, operated by the NIST nSoft consortium, at the National Institute of Standards and Technology Center for Neutron Research (NCNR). The incoming neutron wavelength was set to 5 and 12 Å for the collection of mid to high q and low q data, respectively. Furthermore, the sample-to-detector distance (SDD), as well as the detector offset, was varied to collect a range of q values for the two wavelength settings (q values ranging from 0.0035 to 0.5 $Å^{-1}$). The total collection time for each sample was approximately 3 h. Prior to the beginning neutron scattering experiments, the hybrid membranes were equilibrated in H_2O, D_2O, or a mixture of both for at least 24 h. The hydrated films were then mounted in a zero-gap sample cell with quartz windows. After completion of the scattering experiments, the hydrated film thickness was measured using a micrometer. Film thicknesses were taken as the average of at least three measurements on the sample. The measured intensity from SANS was converted to absolute intensity by correcting for transmission and background scattering. The SANS data were reduced using software developed at the NIST Center for Neutron Research.[46]

Vanadium Crossover Analysis: The experimental set-up used to investigate the crossover of vanadium ions through pristine and modified Nafion membranes is shown in Figure 1a. As seen in Figure 1a, the reservoir above the Nafion membrane was filled with a solution of 1.5 mol L^{-1} $VOSO_4$ in 3 mol L^{-1} H_2SO_4, while the reservoir below the membrane was filled with a solution of 1.5 mol L^{-1} $MgSO_4$ in 3 mol L^{-1} H_2SO_4. Aliquots were taken from the bottom reservoir at regular time intervals, and the concentration of vanadium ions, specifically the vanadium(IV) ion, was measured using an UV–vis spectrometer (PerkinElmer Lambda 950) in the 300 nm to 1100 nm wavelength range. All crossover experiments were carried out at room temperature.

High-Resolution Analytical Scanning Transmission Electron Microscopy: Cross-sectional TEM samples were prepared by embedding small pieces of membrane into the Spurr resin (purchased from SPI Supplies) and curing the resin at 65 °C for 12 h. Ultrathin (80 to 120 nm thick) sections were cut by using a diamond knife in the ultramicrotome (Leica Ultracut UCT) at room temperature. Conventional (amplitude contrast) and high-resolution (phase contrast) transmission electron microscopy (CTEM/HRTEM) and scanning transmission electron microcopy (STEM) imaging, selected-area electron diffraction (SAED), and energy-dispersive X-ray (EDX) spectroscopic analyses of the cross-sections of Nafion–SiO_2 composite membranes were performed in a Schottky field-emission FEI Titan 80–300 analytical S/TEM with a point-to-point resolution of 0.19 nm and information limit below 0.1 nm, equipped with S-TWIN objective lenses and operating at 300 kV accelerating voltage. For high spatial resolution nanoanalysis in STEM mode with 0.14 nm to 0.2 nm diameter probes, the instrument was supplied with a Fischione 3000 model high-angle annular dark-field (HAADF) detector, FEI bright-field (BF-) and ADF-STEM detectors, and a 30 mm^2 EDAX Si/Li EDX detector with a 0.13 s rad acceptance angle. To ensure optimal counting rates, the specimens were tilted 15° toward the EDX detector. To reduce a beam-induced damage of the specimens, the lowest electron beam dose rates down to a few e nm^{-2} s^{-1}, as well as beam blanking between acquisitions during imaging and analyses were used.

Acknowledgements

The authors would like to thank Dr. Ronald Jones and nSoft (www.nist.gov/nsoft) for the use of their beam line and Dr. Jeffrey Fagen for his assistance with UV–vis training. The authors would also like to thank Dr. Joseph Dura for his insightful and fruitful discussions regarding the SANS data on the Nafion hybrid membranes, as well as the National Research Council (NRC) Research Associateship Program (RAP) for their financial support for this work.

Received: March 19, 2015
Revised: April 15, 2015
Published online: May 21, 2015

[1] Z. Yang, J. Zhang, M. C. W. Kintner-Meyer, X. Lu, D. Choi, J. P. Lemmon, J. Liu, *Chem. Rev.* **2011**, *111*, 3577.
[2] X. Li, H. Zhang, Z. Mai, H. Zhang, I. Vankelecom, *Energy Environ. Sci.* **2011**, *4*, 1147.
[3] J. Xi, Z. Wu, X. Qiu, L. Chen, *J. Power Sources* **2007**, *166*, 531.
[4] Equipment and instruments or materials are identified in the paper in order to adequately specify the experimental details. Such identification does not imply recommendation by the National Institute of Standards and Technology (NIST), nor does it imply the materials are necessarily the best available for the purpose.
[5] R. Zaffou, W. N. Li, M. L. Perry, in *Polymers for Energy Storage and Delivery: Polyelectrolytes for Batteries and Fuel Cells* (Eds: K. A. Page, C. L. Soles, J. Runt), ACS Symposium Series, American Chemical Society, Washington, DC **2012**.
[6] Z. Mai, H. Zhang, X. Li, S. Xiao, H. Zhang, *J. Power Sources* **2011**, *196*, 5737.
[7] X. Teng, Y. Zhao, J. Xi, Z. Wu, X. Qiu, L. Chen, *J. Membr. Sci.* **2009**, *341*, 149.
[8] S. Sang, Q. Wu, K. Huang, *J. Membr. Sci.* **2007**, *305*, 118.
[9] Q. Luo, H. Zhang, J. Chen, P. Qian, Y. Zhai, *J. Membr. Sci.* **2008**, *311*, 98.
[10] Q. Luo, H. Zhang, J. Chen, D. You, C. Sun, Y. Zhang, *J. Membr. Sci.* **2008**, *325*, 553.
[11] J. Xi, Z. Wu, X. Teng, Y. Zhao, L. Chen, X. Qiu, *J. Mater. Chem.* **2008**, *18*, 1232.
[12] K. A. Mauritz, R. M. Warren, *Macromolecules* **1989**, *22*, 1730.
[13] D. H. Jung, S. Y. Cho, D. H. Peck, D. R. Shin, J. S. Kim, *J. Power Sources* **2002**, *106*, 173.
[14] P. L. Shao, K. A. Mauritz, R. B. Moore, *Chem. Mater.* **1995**, *7*, 192.
[15] K. A. Mauritz, J. T. Payne, *J. Membr. Sci.* **2000**, *168*, 39.
[16] Q. Deng, R. B. Moore, K. A. Mauritz, *Chem. Mater.* **1995**, *7*, 2259.
[17] M. Vijayakumar, B. Schwenzer, S. Kim, Z. Yang, S. Thevuthasan, J. Liu, G. L. Graff, J. Hu, *Solid State Nucl. Magn. Reson.* **2012**, *42*, 71.
[18] B. P. Ladewig, R. B. Knott, A. J. Hill, J. D. Riches, J. W. White, D. J. Martin, J. C. Diniz da Costa, G. Q. Lu, *Chem. Mater.* **2007**, *19*, 2372.
[19] K. A. Mauritz, R. F. Storey, C. K. Jones, in *Multiphase Polymer Materials: Blends, Ionomers and Interpenetrating Networks* (Eds: L. A. Utracki, R. A. Weiss), ACS Symposium Series, American Chemical Society, Washington, DC **1989**.
[20] K. A. Mauritz, I. D. Stefanithis, *Macromolecules* **1990**, *23*, 1380.
[21] X. Teng, Y. Zhao, J. Xi, Z. Wu, X. Qiu, L. Chen, *J. Power Sources* **2009**, *189*, 1240.
[22] K. A. Mauritz, I. D. Stefanithis, S. V. Davis, R. W. Scheetz, R. K. Pope, G. L. Wilkes, H. H. Huang, *J. Appl. Polym. Sci.* **1995**, *55*, 181.
[23] Q. Deng, R. B. Moore, K. A. Mauritz, *J. Appl. Polym. Sci.* **1198**, *68*, 747.
[24] V. Tricoli, *J. Electrochem. Soc.* **1998**, *145*, 3798.
[25] P. Trogadas, E. Pinot, T. F. Fuller, *Electrochem. Solid-State Lett.* **2012**, *15*, A5.
[26] A. Kusoglu, D. Kushner, D. K. Paul, K. Karan, M. A. Hickner, A. Z. Weber, *Adv. Funct. Mater.* **2014**, *24*, 4763.
[27] G. Gebel, J. Lambard, *Macromolecules* **1997**, *30*, 7914.
[28] L. Rubatat, A. Laure Rollet, G. Gebel, O. Diat, *Macromolecules* **2002**, *35*, 4050.
[29] T. D. Gierke, G. E. Munn, F. C. Wilson, *J. Polym. Sci.: Polym. Phys. Ed.* **1981**, *19*, 1687.
[30] M. Fujimura, T. Hashimoto, H. Kawai, *Macromolecules* **1981**, *14*, 1309.
[31] H.-G. Haubold, Th. Vad, H. Jungbluth, P. Hiller, *Electrochim. Acta* **2001**, *46*, 1559.
[32] M.-H. Kim, C. J. Glinka, S. A. Grot, W. G. Grot, *Macromolecules* **2006**, *39*, 4775–4787.
[33] K. Schmidt-Rohr, Q. Chen, *Nat. Mater.* **2008**, *7*, 75.
[34] J. A. Dura, V. S. Murthi, M. Hartman, S. K. Satija, C. F. Majkrzak, *Macromolecules* **2009**, *42*, 4769.
[35] S. C. DeCaluwe, P. A. Kienzle, P. Bhargava, A. M. Baker, J. A. Dura, *Soft Matter* **2014**, *10*, 5763.
[36] B. Loppinet, G. Gebel, C. E. Williams, *J. Phys. Chem. B* **1997**, *101*, 1884.
[37] R. Buzzoni, S. Bordiga, G. Ricchiardi, G. Spoto, A. Zecchina, *J. Phys. Chem.* **1995**, *99*, 11937.
[38] S. K. Young, S. F. Trevino, N. C. Beck Tan, *J. Polym. Sci., Part B: Polym. Phys.* **2002**, *40*, 387.
[39] S. A. Eastman, S. Kim, K. A. Page, B. W. Rowe, S. Kang, S. C. De Caluwe, J. A. Dura, C. L. Soles, K. G. Yager, *Macromolecules* **2012**, *45*, 7920.
[40] S. Yakovlev, N. P. Balsara, K. H. Downing, *Membranes* **2013**, *3*, 424.
[41] M. A. Dresch, B. R. Matos, F. C. Fonseca, E. I. Santiago, M. Carmo, A. J. C. Lanfredi, S. Balog, *J. Power Sources* **2015**, *274*, 560.
[42] J. M. Kropka, V. Garcia Sakai, P. F. Green, *Nano Lett.* **2008**, *8*, 1061.
[43] A. P. Holt, P. J. Griffin, V. Bocharova, A. L. Agapov, A. E. Imel, M. D. Dadmun, J. R. Sangoro, A. P. Sokolov, *Macromolecules* **2014**, *47*, 1837.
[44] H. Oh, P. F. Green, *Nat. Mater.* **2009**, *8*, 139.
[45] T. A. Zawodzinski, Jr. , M. Neeman, L. O. Sillerud, S. Gottesfeld, *J. Phys. Chem.* **1991**, *95*, 6040.
[46] S. R. Kline, *J. Appl. Crystallogr.* **2006**, *39*, 895.